1-1-2014

Behaviour of hollow core square reinforced concrete columns wrapped with CFRP with different fibre orientations

Muhammad N. Hadi
University of Wollongong, mhadi@uow.edu.au

T D. Le
University Of Wollongong

Behaviour of hollow core square reinforced concrete columns wrapped with CFRP with different fibre orientations

Abstract

Results of testing twelve hollow core square reinforced concrete columns wrapped with Carbon fibre 33 reinforced polymer (CFRP) are presented. The effect of fibre orientation on the performance of specimens 34 under concentric and eccentric loads was investigated. Twelve specimens were divided into four groups with three 36 specimens each. The specimens in the first reference group were unwrapped, while the specimens in the 37 remaining groups were wrapped with CFRP of different wrap combinations of three fibre orientations.The specimens in each group were tested 39 under three eccentricities: 0 (concentric), 25, and 50 mm up to failure. Test results show that all wrap- 40 ping configurations increased both the strength and ductility of hollow core square reinforced concrete 41 columns. However, the increase of compressive strength was marginal. The columns, which were 42 wrapped exclusively with hoop configuration, proved to have the greatest ductility. Axial load-bending 43 moment P- M interaction diagrams of each group were drawn based on the experimental results and 44 compared with theoretical calculations.

Keywords

cfrp, different, fibre, orientations, core, square, behaviour, reinforced, hollow, concrete, columns, wrapped

Disciplines

Engineering | Science and Technology Studies

Publication Details

Hadi, M. N. & Le, T. D. (2014). Behaviour of hollow core square reinforced concrete columns wrapped with CFRP with different fibre orientations. Construction and Building Materials, 50 (January), 62-73.

Behaviour of Hollow Core Square Reinforced Concrete Columns Wrapped with CFRP with Different Fibre Orientations

M.N.S. Hadi and T.D. Le

School of Civil, Mining and Environmental Engineering, University of Wollongong, Wollongong, NSW 2522, Australia

Research Highlights

This paper presents results of testing twelve reinforced concrete hollow core columns wrapped with FRP. The aim of the tests was to investigate the effect of fibre orientation on the behavior of these columns. All the specimens were made of reinforced concrete with the same amount of internal steel reinforcement and were designed according to the requirements of the Australian Standard AS 3600-2009. The specimens had square cross-section with 200 mm side dimension, 800 mm height, and a 80x80 mm hole at their center. All corners of the specimens were rounded to 32 mm radius to prevent premature failure of FRP wraps due to stress concentration. The columns were tested under different eccentricities.

The following conclusions are drawn:

The fibre in the hoop direction can significantly increase the ductility of hollow core square reinforced concrete columns under concentric or eccentric loading. However, the increment of the compressive strength of FRP-confined hollow core columns is marginal.

The combination of $\pm 45^{o}$ oriented CFRP layers and one hoop layer was expected to have the largest ductility. However, it did not show any significant increase in deflections of the columns under both concentric and eccentric testing.

The analysis of results showed that the stress-strain model developed by Mander at al. (1998) for solid rectangular columns is applicable for hollow core columns wrapped with FRP. The model results are agreeable with the experimental results.

Behaviour of Hollow Core Square Reinforced Concrete Columns Wrapped with CFRP with Different Fibre Orientations

M.N.S. Hadi * and T.D. Le

School of Civil, Mining and Environmental Engineering, University of Wollongong, Wollongong, NSW 2522, Australia

Abstract:

Results of testing twelve hollow core square reinforced concrete columns wrapped with Carbon fibre reinforced polymer (CFRP) are presented. The effect of fibre orientation on the performance of specimens under concentric and eccentric loads was investigated. Twelve specimens (200 mm x 200 mm in cross-section, 800 mm in height and having an 80 mm square hole) were divided into four groups with three specimens each. The specimens in the first reference group were unwrapped, while the specimens in the remaining groups were wrapped with CFRP of different wrap combinations of three fibre orientations (0^o, 45^o, and 90^o with respect to the circumferential direction). The specimens in each group were tested under three eccentricities: 0 (concentric), 25, and 50 mm up to failure. Test results show that all wrapping configurations increased both the strength and ductility of hollow core square reinforced concrete columns. However, the increase of compressive strength was marginal. The columns, which were wrapped exclusively with hoop configuration, proved to have the greatest ductility. Axial load-bending moment P-M interaction diagrams of each group were drawn based on the experimental results and compared with theoretical calculations.

Keywords: CFRP, RC columns, hollow square sections, fibre orientation, eccentricity

* Corresponding author. Tel.: +61-2-4221-4762; fax +61-2-4221-3238.
E-mail address: mhadi@uow.edu.au

1. Introduction

Several studies have shown that fibre reinforced polymer (FRP) is efficient in strengthening concrete columns for both strength and ductility. These studies mostly focused on testing solid cross-section columns, which are wrapped with FRP in the hoop direction. When the concrete is subjected to axial compression, it tends to expand. This lateral expansion is restrained by the activation of FRP stressing in tension. Thereby, FRP-confined concrete core of solid section columns is subjected to triaxial compression, which increases the strength of concrete. In addition, FRP delays the failure of concrete core leading to increasing the column's ductility. Meanwhile the response of hollow core columns under compressive loading is significantly different from that of solid columns due to the existence of a void part. The concrete in a FRP-confined hollow core column is in a state of biaxial stress. As the strength of FRP is much greater than the capacity of the concrete core, under large loads the concrete may crumple inwardly resulting in an ineffective confinement. Review of literature shows that limited numbers of studies were undertaken to investigation the behaviour of hollow core columns, especially for hollow core non-circular cross-sections in which the confinement pressure is non-uniform and complicated. This paper deals with hollow core square reinforced concrete column, and fibre orientation is the main study parameter. The variation in fibre orientation that affects the strength, ductility and failure modes of the specimens was studied and discussed herein.

1.1 FRP in strengthening solid core columns

Wrapping FRP transversely with respect to column's axial axis was mostly used in previous studies. These studies proved that circumferential FRP wraps provide considerable confinement pressure to the concrete core under compressive loads delaying the crushing of concrete and buckling of longitudinal steel reinforcement, as a result, increasing the

compressive strength and deformation capacity of the column. However, these enhancements are only achieved when a column is tested concentrically or when the eccentricity of the load is small. When the eccentricity is large, the load carrying capacity is significantly reduced because both axial action and bending action are induced. Li and Hadi [1], Hadi [2,3] conducted experiments on circular concrete columns under different eccentricities. Results of these studies show that external confinement with FRP improves the performance of columns under eccentric loading. However, while the gain in ductility was distinctive, the strength was only enhanced to some extent when an eccentric load was applied. In fact, under eccentric compressive loading, columns bend producing an additional bending moment (secondary moment) on the column. The increase in the applied load results in lateral deflection increases and the total eccentricity of the applied load is thereby increased. This in turn increases the internal moment of the column and causes compressive strength capacity reduction.

FRP confinement leads to greater slenderness in the column [4], leading to increased lateral bending acting on the column. To resist such bending moment, vertical FRP layers were provided and the outcomes show to be very good from some experimental results. Hadi [5] tested circular concrete columns externally confined with FRP but vertical FRP wraps were added. The author concluded that the adding vertical CFRP straps improved significantly the performance of the columns for both strength and ductility under eccentric loading. Hadi and Widiarsa [6] conducted an experimental program on solid, square, reinforced concrete columns, and similar results were reported. In fact, the benefit of longitudinal wraps is more obvious with the increase in eccentricity. Tan [7] also confirmed that increasing the amount of longitudinal fibre sheets leads to enhancement in strength and ductility of the solid, square, concentrically loaded columns. However, this increase would be possible only if they are adequately restrained from outward buckling by transverse fibre

sheets.

Wrapping FRP in other directions was also studied by several researchers. Rochette and Labossiere [8] used fibres oriented at $\pm 15^{o}/0^{o}$ to wrap square concrete columns. Mirmiran and Shahawy [9] applied $\pm 15^{o}$ fibres from the hoop direction in their concrete-filled FRP tubes. In the study by Pessiki et al. [10], $0^{o}\pm 45^{o}$ oriented fibres were used to wrap both small and large scale square and circular concrete columns. However, these specimens were not extensively analyzed in both strength and ductility aspects. Li et al. [11] tested concentrically FRP-confined concrete cylinders (152.4 mm diameter and 304.8 mm height) to study the effect of fibre orientation on their structural behaviour. A variety of fibre orientations with different thicknesses were used in their study. It was found that the strength, ductility, and failure mode of the confined cylinders depend on the CFRP wrapping orientation and layer thickness. Wrapping FRP at a certain angle in between the hoop direction and the vertical direction may result in strength lower than that of a column wrapped with FRP in the hoop direction only. Specimens wrapped with 45^{o} FRP showed a slight increase in the axial strain. As stated by the authors, the main reason for this slight increase in axial displacement was insufficient provision of FRP. Sadeghian et al. [12] also investigated the effect of fibre orientation on concrete cylinders (150 mm diameter and 300 mm height) under uniaxial compressive loading. They concluded that longitudinal fibres have no significant effect on strength and ductility of specimens under concentric loading meanwhile the angle orientations influenced significantly the enhancement of ductility and energy dissipation of columns.

Parvin A, Jamwal [13,14], and recently Hajsadeghi et al. [15] used the finite element analysis method to study the behaviour of FRP-confined concrete columns for changes in FRP ply configuration. The authors concluded that the rate of increase in ductility is highest

for fibre oriented at an angle other than the hoop and longitudinal orientations. This is noteworthy as the ductility is an important parameter of a member allowing the material to undergo large plastic deformation without failure in a brittle and abrupt manner, particularly during large earthquakes where forces are expected to exceed the yield strength of the material.

1.2 FRP in strengthening hollow core columns

Recently, several studies have investigated hollow core columns. Lignola et al. [16] conducted a study on hollow square columns wrapped with CFRP in the hoop direction and tested them under various eccentricities. The test results showed that horizontally oriented wraps could improve strength and ductility of hollow core square columns under eccentric loading. However, the strength enhancement was more pronounced for specimens loaded with a smaller eccentricity. Ductility increases with the increase of eccentricity. Yazici and Hadi [17] performed a study on hollow core circular concrete columns. CFRP layers in the transverse direction were also used in their experiments to wrap specimens. Similar conclusions were drawn by the authors that strength improvement of CFRP wrapped columns under concentric load was higher than eccentrically loaded CFRP wrapped columns. When eccentricity was larger, the increase in strength was reduced meanwhile that for ductility increased. Kusumawardaningsih and Hadi [18] studied the effectiveness of FRP confinement on hollow high strength RC columns. Both circular and square columns with either circular or square hollow core were cast and tested under axial concentric loading. The FRP in the hoop direction was also used to wrap specimens in their experiment. It was found that FRP confinement increased the strength and ductility of hollow core high strength RC columns. Hollow core columns having circular holes showed better performance as compared to columns having square holes.

Internally confined hollow (ICH) RC columns were suggested and investigated by Han et al. [19,20]. In an ICH RC column, a tube is placed at the inner face of the column to confine the concrete wall element. The test results revealed that the internal confinement existed and made the concrete in the state of triaxial confinement. The internal confinement prevented the spalling of the inner face of the concrete, and increase in the strength of the concrete as a result of in the state of triaxial confinement.

There have also been studies on confining the concrete of both outer and inner face of hollow concrete columns in order to make the concrete under triaxial confinement. Hybrid FRP-concrete-steel double-skin tubular columns (referred to as DSTCs) have been introduced Teng et al. [21] for one of such purposes. A hybrid DSTC consists of a layer of concrete sandwiched between an outer tube made of FRP and an inner tube made of steel. Several studies have been carried out on this type of structure [21-26]. These test results confirm that the concrete in the new column is very effectively confined by the two tubes. The FRP tube offers mechanical resistance primarily in the hoop direction to confine the concrete and to enhance the shear resistance of the member; the steel tube acts as the main longitudinal reinforcement and prevents the concrete from inward spalling. However, this type of structure is not of interest to the present study.

From the above review, it is shown that no study has been conducted on the investigation of the behaviour of hollow core columns wrapped with different fibre orientations under various eccentricities.

2. Experimental program

2.1 Specimen preparation

In order to investigate the effect of ply configuration on the behaviour of hollow core RC

columns confined with FRP, a total of twelve specimens were designed, cast, and tested to failure. All the specimens were made of reinforced concrete with the same amount of internal steel reinforcement and were designed according to the requirements of the Australian Standard AS 3600-2009 [27]. All tests were carried out at the laboratories of the School of Civil, Mining, and Environmental Engineering, University of Wollongong.

The specimens had square cross-section with 200 mm side dimension, 800 mm height, and a 80x80 mm hole at their center. All corners of the specimens were rounded to 32 mm radius to prevent premature failure of FRP wraps due to stress concentration. The specimens' dimensions were chosen based on the available equipment. The specimens were considered to be short columns. 60 mm wall thickness was designed to ensure a clear concrete cover of 20 mm was maintained at both outer and hole faces of the column as specified in AS 3600-2009 [27]. With the wall width-to-thickness ratio of 1.33, which is less than 15, the failure mode of the compression flange will be controlled by crushing of the concrete instead of local buckling [28] . The size effect, however, is not considered in this study. Two types of steel reinforcement were used. 12 mm diameter deformed bars N12 (500 MPa nominal tensile strength) were used for longitudinal reinforcement. 6 mm diameter plain bars R6 (250 MPa nominal tensile strength) were used for transverse reinforcement and were placed at 100 mm spacing. Details of the dimensions and reinforcement are given in Fig. 1.

For all columns, four strain gages were bonded at mid-height of the four longitudinal steel bars, and two strain gages were bonded on the tie at mid-height of the column. These strain gages were used to check the strain in the steel reinforcement.

A wooden formwork having twelve square holes was used to cast the specimens. To create the inside hole, twelve 80 mm by 80 mm wooden boxes were also made and placed at the center of each mold. Four foam arches with 32 mm radius were placed at the four corners of

each hole to produce round corners for the specimens. 40 MPa nominal compressive strength concrete was used in this experiment and was supplied by a local supplier in one batch of concrete. The concrete had 130 mm slump ensuring its workability. The concrete was then placed into the formwork at three stages. At each stage, vibration was carried out using two vibrators to ensure compaction of concrete. Cylinders (100 mm diameter and 200 mm height) were also cast to determine the properties of concrete.

After casting, the specimens were cured in their forms in moist conditions. Wet hessian rugs were placed on the top of all the specimens and were watered twice a day to keep them moist. The formwork was removed after 21 days of casting the specimens.

2.2 Wrapping and curing FRP

Before wrapping FRP, the concrete surface was prepared carefully. The concrete surface of all specimens was found to be intact after removing the formwork. Therefore, there was no need for repair or patch, except the surface at corners due to using foam. These locations were then ground using a grinder and a steel brush to make them smooth.

Unidirectional CFRP fibre sheets (CARBON-UNI340GM-75MM) were used in this experimental program to wrap the specimens using wet layup system. The nominal width and thickness of the CFRP sheet were 75 mm and 0.45 mm, respectively. The properties of FRP were determined from the FRP coupon tests according to ASTM D7565 [29]. FRP coupons consisting of one, two and three parallel CFRP layers were prepared and tested. Test results are shown in Table 1. The adhesive was mixed from epoxy resin and slow hardener at a ratio of 5:1 as recommended by the manufacturer.

The twelve specimens were sub-divided into four groups with three specimens each. The specimens of the first group (RC Group) without any FRP wraps served as reference

specimens. The specimens of the second group (HF Group) were laterally wrapped with three CFRP layers with respect to the specimen's axial axis. The specimens of the third group (VHF Group) were vertically wrapped with one CFRP layer along the specimen's axial axis, and then horizontally wrapped with two CFRP layers. All the specimens of the last group (AHF Group) were wrapped with two CFRP layers oriented at $\pm 45^0$ with respect to specimen's axial axis, and then horizontally wrapped with one layer of CFRP.

The wrapping procedure was done as follows. The surface of the specimens was coated with a thin layer of epoxy resin first, and then the first layer of CRRP was applied at the design orientation. The first layer of FRP was then coated with epoxy again before the application of the second FRP layer. The process was repeated until all the design FRP layers were applied. An overlap of 100 mm was made in the last revolution and was applied only in the hoop direction. Two extra lateral FRP layers and 75 mm length vertical FRP layers were applied at the ends of all specimens in order to protect the two ends against premature failure due to stress concentration and from early cracking on the tension sides of the ends under eccentric loading. After completing wrapping, all specimens were left for at least 14 days for binder curing.

2.3 Preliminary testing

Preliminary testing included testing concrete cylinders, reinforcing bars. Determination of concrete properties was conducted according to the Australian Standards AS 1012.8 [30] and AS 1012.9 [31] for concrete cylinders. The cylinder dimensions were 100 mm diameter and 200 mm height. The average 28 day concrete compressive strength was 38 MPa. The tensile testing method according to Australian Standard AS 1391 [32] was used to determine the reinforcing steel properties. The average tensile strength and tensile strain of N12 were 587 MPa and 0.0029, respectively. Those for R6 were 538 MPa and 0.00269, respectively.

2.4 Testing specimens

Testing of the specimens was conducted at the High Bay laboratory, University of Wollongong using the Dension 5000 kN compression testing machine. From each group, the specimens were tested as columns at eccentricities of 0 (concentric), 25 mm and 50 mm. These specimens were denoted by the group label accompanied with 0, 25 and 50 at the end. For example, Specimens RC-0, RC-25, RC-50 denote that these specimens are in Group RC (reference columns) and were tested under an eccentricity of 0, 25, and 50 mm, respectively. The test matrix is given in Table 2.

Square, steel loading caps were used in testing all specimens (Fig. 2). The loading cap consists of two parts: a 50 mm thick steel plate, called adaptor plate, which exerts the load to the column, and a 25 mm thick steel plate with a circular roll joint, which was only used in eccentric loading tests that ensure rotation capacity of column's ends during test. As such, the boundary condition of the eccentrically loaded columns was pin-pin (refer to Fig. 3). Details of the loading caps are described in Hadi and Widiarsa [6]. High strength plaster was placed in the caps (to create a level surface between the plate and the bottom or top ends of the specimens) and left to set for at least 45 mins before testing. The bottom loading cap was cantered using a rig holding the column in place. A forklift was used to place the specimen in the testing machine. The top loading cap was placed as the column was lifted into place. A photo of a typical compression testing is shown in Fig. 4.

In order to measure the lateral displacement of the columns, a laser triangulation sensor was placed horizontally at the front of the protective perspex shield with a small cutout hole for the sensor. A data taker was used to link the testing machine with a computer to detect the loading ram that exerts the load, the longitudinal deflection, and the lateral deflection from the laser triangulation sensor. Testing commenced under displacement controlled condition.

All tests were conducted at a rate of 0.3 mm/min.

3. Results and discussions

Table 3 shows results of testing all columns. The ultimate displacement was taken at the point when the corresponding axial load was equal to 85% of the maximum load for unwrapped specimens and at the point when the FRP ruptured for confined specimens. Similar to solid reinforced concrete columns, externally wrapping CFRP can increase the performance of hollow core RC columns, in terms of strength and ductility. The gain in strength is significant for columns wrapped exclusively with hoop FRP layers (HF columns) under concentric loading or when the eccentricity of the load is small (25 mm). When the eccentricity is large (50 mm), the strength gain is more considerable for columns with the presence of vertical or $\pm 45^{o}$ CFRP wraps (VHF and AHF columns). In addition, hoop orientation wrapping of HF columns increased their ductility significantly compared with unwrapped columns, and columns in Groups VHF and AHF.

3.1 Behaviour of unwrapped specimens

The unconfined columns (Group RC) showed the highest load carrying capacity when tested under concentric loading. When eccentricities were introduced, the maximum load carrying capacity decreased significantly due to bending moment effect. These columns did not suffer any large strain after reaching the maximum load. In fact, they failed in a brittle manner characterized by peeling off the concrete and outward buckling of the steel bars within two adjacent ties in the compression side for all columns. Horizontal cracks were formed in the tension side at the failure position of the columns tested under eccentric testing.

3.2 Behaviour of specimens of the HF group

Wrapping columns with three layers in the hoop direction was the most efficient method

for increasing the strength and ductility of columns for both concentric and eccentric loading. Specimen HF-0 showed 11% increase in maximum load compared to the reference specimen RC-0 in concentric testing. Specimens HF-25 and HF-50 achieved 25% and 9% increases, respectively compared with the corresponding reference specimens. Specimen HF-0 was expected to gain the highest applied load of the four columns tested concentrically, however a premature failure was observed. After examining the tested HF-0 specimen carefully, it was found that the concrete had spalled at a corner at the surface of the top end where the longitudinal steel bar was exposed. It is to be noted that one longitudinal steel bar was moving upward during casting this specimen. This movement may be the reason for this exposure. Therefore, the concrete cover at the top of this longitudinal steel bar was just 4 mm instead of the required 20 mm. This occurrence caused high stress concentration, resulting in premature damage at the top end of the column at this corner.

In terms of ductility, Figures 5 to 7 show clearly that hoop layers can substantially extend axial displacement as well as lateral displacement of the columns under concentric and eccentric loading. Table 4 shows the ductility calculation for all specimens. In this study ductility was calculated based on axial displacement behaviour which was suggested by GangaRao et al. [33], i.e. the ductility is equal to the ratio of the axial displacement at 85% maximum load (post-yielding point) $\Delta_{85\%Pmax}$ and the axial displacement at yield load Δ_y. Hoop orientation wrapping of Specimen HF-0 increased the axial displacement 4.7 times that of the reference specimen RC-0, and around 2.4 times those of Specimens VHF-0 and AHF-0. Under eccentric loading, these comparisons are even larger. Specimen HF-50 showed a ductility 7.4 times larger than Specimen RC-50 and about 3.4 times larger than Specimens VHF-50 and AHF-50. The ductility of Specimen HF-25 was not calculated due to an accident that occurred with the machine as testing commenced. The applied load suddenly increased with a very high speed rate and in about 16 seconds, 1250 kN force was applied before the

test was stopped. The load data recorded from the computer showed that the applied load reached the maximum value and then started decreasing. It was decided to start the test again, but some cracks were already found on the FRP layers. The maximum load the column achieved was only about 80% of the previous value recorded during the accident. The axial and lateral displacements however, were still very large as shown in Fig. 5. Therefore, CFRP layers in the hoop direction were efficient in delaying premature failure of the columns due to the spalling of concrete and buckling of steel bars at yield load.

It is worthy to note that when eccentricity was large, the gain in strength of HF columns decreased, whereas the gain in ductility increased. This result is due to FRP in this wrapping method only working in the hoop direction and there is no effect in preventing the loss of strength caused by bending moment.

Specimens of Group HF failed in a sudden, dangerous manner. When the applied load increased to large enough values, small cracking sounds were heard. After the maximum load, the load carrying capacity of the columns slightly reduced while the deflection significantly increased allowing HF columns to achieve large ductility. When the deflection was large enough, the cracking sounds increased and the FRP ruptured with a loud explosive noise as it reached its ultimate strain. The failure position of FRP layers of Specimens HF-0 and HF-50 was determined to be about 160 mm - 200 mm from the top end and that for Specimen HF-25 was near the mid-height of the column. All of these FRP layers ruptured at a corner of the column due to stress concentration at corners of non-circular cross-section columns. Failure modes of all specimens are shown in Fig. 8.

3.3 Behaviour of specimens of the VHF and AHF groups

The behaviours of VHF and AHF columns were quite similar in both concentric and eccentric loading, especially with regards to ductility. Both of these wrapping schemes

improved slightly the ductility of the columns. The combination of two ±45^{o} oriented CFRP layers and one hoop CFRP layer of AHF columns were expected to show the largest ductility compared to the other schemes, but their gain in ductility was only around 1.6 to 2.1 times larger than the corresponding reference specimens. These results are similar to those of Sadeghian et al. [12] which were conducted on solid plain concrete cylinders. The combination of transverse and angle oriented layers is not effective in enhancing the ductility and energy absorption. Meanwhile, Sadeghian et al. [12] confirmed the significant increase in ductility for cylinders wrapped with only ±45^{o} orientations.

With respect to strength, as expected, the gain in strength of these specimens increased when the eccentricity increased due to the contribution of the vertical and angle wraps. When the columns were tested concentrically, there was no contribution of vertical and angle layers resulting in only a slight increase in the strength, which in fact came from the hoop layers (Table 3). At an eccentricity of 50 mm, the contribution of vertical and angle layers became clearer. The increase in strength of Specimens VHF-50 and AHF-50 were even greater than that of Specimen HF-50 (i.e. 9% for HF-50, meanwhile 18% and 14% for VHF-50 and AHF-50, respectively). Therefore, the presence of vertical and angle CFRP orientation is clearly efficient in resisting bending moments due to eccentricities, which results in premature failure of RC columns. This achievement is similar to Hadi [5] and Hadi and Widiarsa [6] in testing solid reinforced concrete columns when vertical FRP layers were added.

Specimens in Groups VHF and AHF also failed in a sudden and explosive manner. When the applied load was large enough, small cracking sounds were heard. A bulging deformation on the outer hoop FRP layer in the compression side was also observed. After the maximum load, the load carrying capacity of VHF and AHF specimens reduced significantly. The rupture of the outer hoop layers caused a loud explosive noise and the load dropped.

All VHF columns failed at a position approximately 130 mm from the top end. With the exception of Specimen VHF-0, the rupture of FRP in VHF specimens (VHF-25 and VHF-50) occurred in the middle, on the side of the column, not at the corner. After examining inside the hole of these specimens, it was found that the concrete at the inner corners broke in a way that tends to make the cross-section of the hole at failure position circular, as a result, the concrete in the middle of the compression side expanded outwards causing the FRP failure near the middle side of the column.

For AHF columns, the rupture of FRP started from the corner and further developed into an approximate 45^0 downward angle in the compression side of the column. The failure positions varied between 130 mm to 200 mm from the bottom end of the columns.

All the specimens failed near the ends, not the desired midspan. Possible reason is the stress concentration at the boundaries.

4. Theoretical considerations

In order to predict the axial loading capacity and combined axial compression and flexure, P-M interaction diagrams were drawn based on theoretical calculations for both unconfined RC columns and FRP-confined columns.

For unconfined RC columns, P-M diagrams can be developed by satisfying strain compatibility and force equilibrium using the model for the stress-strain behaviour of conventional RC columns. The detailed procedure is based on Warner et al. [34].

A similar procedure was applied to construct the P-M diagram for FRP-confined specimens. However, the stress-strain model for unconfined concrete was replaced by a stress-strain model for FRP-confined concrete. When observing the load-axial displacement

response diagrams, it is noted that all of FRP-confined specimens exhibited stress-strain curves of descending type. In these curves, the maximum confined concrete strength f'_{cc} was greater than the unconfined concrete strength f'_{co}. The axial strength of confined concrete at ultimate axial strain f'_{cu} fell below f'_{co}. These curve types are similar to the stress-strain curves originally developed by Mander et al. [35] for steel confined concrete which was adopted by ACI 440.2R-02 [36] with modifications for FRP-confined concrete. ACI 440.2R-08 [37] adopted the stress-strain model proposed by Lam and Teng [38] for FRP-confined concrete. However, this model is only applicable for a nondescending second branch in the stress-strain performance, in which, the maximum value of f'_{cc} is reached at the same time with the ultimate strain of FRP (the failure strain of FRP) ε_{ccu}. To assure an ascending second branch of the stress-strain curve a minimum level of confinement is required, i.e the ratio f_l / f'_c should not be less than 0.08 [37] or 0.07 [38], below which the FRP is considered to result in no enhancement in the compressive strength of concrete, i.e $f'_{cc}/f'_{co} = 1$ if $f_l / f'_c < 0.07$, as suggested by Lam and Teng [38]. In the present study, the maximum confined concrete strength f'_{cc} was higher f'_{co} and was reached before the failure strain of FRP ε_{ccu}. Since there is no specific stress-strain model for FRP-confined hollow core rectangular columns at the present time, the approach presented in ACI 440.2R-02 [36] for solid sections was used herein to calculate compressive strength enhancement. The achieved results show good agreement with the results obtained from the experiments.

The maximum confined concrete strength f'_{cc} and the corresponding strain ε'_{cc} were computed by using Eqs.1 and 2, respectively:

$$f'_{cc} = f'_c \left[2.25\sqrt{1 + 7.9\frac{f_l}{f'_c}} - 2\frac{f_l}{f'_c} - 1.25 \right] \quad (1)$$

$$\varepsilon_{cc}^{'} = \frac{1.71\left(5 f_{cc}^{'} - 4 f_{c}^{'}\right)}{E_c} \quad (2)$$

Where, f'_c is the unconfined concrete strength, E_c is the modulus of elasticity of unconfined concrete, f_l is the confining pressure given in Eq. 3:

$$f_l = \frac{\kappa_a \rho_f f_{fe}}{2} = \frac{\kappa_a \rho_f \varepsilon_{fe} E_f}{2} \quad (3)$$

Where, κ_a is a shape factor, and ρ_f is a reinforcement ratio, which were computed by using Eqs. 4 and 5 for non-circular sections, respectively. f_{fe} is the effective stress in FRP attained from tensile modulus of elasticity of FRP E_f, and effective strain in FRP ε_{fe} at failure section. The efficiency of the FRP jacket is directly related to the strain efficiency factor κ_ε. This factor accounts for the difference between the actual tensile strain at rupture of FRP jacket ε_{fe} and the ultimate strain reported from flat coupon tests ε_{fu}. Carey and Harries [39] reported strain efficiency factor values of 0.13 and 0.16 for one medium-scale and one large-scale CFRP- wrapped square RC columns. Toutanji et al. [40] reported values of 0.16 and 0.26 for two large-scale square RC columns. The value of 0.16 was used in the calculations in this paper.

$$\rho_f = \frac{2nt_f\left(b+h\right)}{A_{net}} \quad (4)$$

$$\kappa_a = 1 - \frac{\left(b-2r\right)^2 + \left(h-2r\right)^2}{3A_{net}\left(1-\rho_g\right)} \quad (5)$$

where n is the number of FRP layers, t_f is the thickness of one FRP layer, b and h are the dimensions of the section, r is the radius of corners of the section, ρ_g is the cross sectional area ratio of the longitudinal steel reinforcement. Note that for Eqs. 4 and 5, the section gross area A_g was replaced by the net area of the hollow section, i.e $A_{net} = A_g - A_{hollow}$, where A_{hollow}

is the area of the hollow part. Eq. 5 was applicable for square sections because the ratio of b and h equal to 1, the size effect was not considered.

The axial load capacity under concentric loading was computed by using Eq. 6:

$$N_{uo} = f'_{cc} A_{net} + f_y A_s \quad (6)$$

where, f_y, A_s are the yield strength and area of longitudinal steel reinforcement, respectively. For columns with the presence of vertical or $\pm 45^{o}$ oriented layers it was assumed that there is no contribution of these layers in concrete core confinement under concentric loading. These contributions were only taken into account in case of eccentric loading, where combined axial compression and flexure took place. The axial load capacity N_u and bending moment M_u were computed by using Eqs. 7 and 8:

$$N_u = (C_c + C_s) - (T + T_{frp}) \quad (7)$$

$$M_u = C_c(d_{PC} - Y_c) + S_c(d_{PC} - d_{sc}) + T(d - d_{PC}) + T_{frp}(d_{frp} - d_{PC}) \quad (8)$$

where, C_c, C_s are the compressive forces in concrete and longitudinal steel reinforcement, respectively. T, T_{frp} are tensile forces in the tensile steel reinforcement and FRP, respectively. d_{PC}, d_{sc}, d, d_{frp} are distances from the extreme compression concrete fibre to the plastic centroid, centroids of compressive steel reinforcement, tensile steel reinforcement and FRP, respectively; and Y_c is the centroid of concrete in the compression region. Rectangular stress block was used to compute the compressive concrete stress f'_{cc} because at the point where the strain in tensile steel reinforcement is equal to zero the neutral axis depth d_n at failure is at the level of the tensile reinforcement. Also, at the balanced failure condition, the neutral axis depth d_n was also noticed to be very close to the flanges that do not contain a large hollow part.

The strain in FRP ε_{frp} was computed using strain compatibility, which was controlled by both confined concrete axial strain ε_{cc} at maximum stress f'_{cc}, and effectively hoop rupture strain of FRP ε_{fe}.

$$\varepsilon_{frp} = \varepsilon_{cc}\left(\frac{d_{frp} - d_n}{d_n}\right) \leq \varepsilon_{fe} \quad (9)$$

In which, d_{frp} is the distance from the extreme compression fibre to the neutral axis, taken equal to the cross-section depth *h.*

The theoretical calculation results are given in Table 5. Fig. 9 shows the theoretical P-M interaction diagrams of all groups of specimens. It can be seen that with the assumption of no contribution of vertical or angle oriented FRP layers under concentric loading, the gain in strength of columns depend on the thickness of hoop FRP layers. The increase in the number of hoop FRP layers can result in an increase in the compression strength capacity of the columns subjected to concentric loads. The test results were of the same tendency (refer to Table 3). The theoretical pure bending moments of RC specimens and HF specimens were equal, meanwhile those for VHF and AHF specimens were significantly greater than RC and HF specimens due to the contribution of the vertical layers and the angle oriented layers close to the tensile steel reinforcement.

Figures 10 - 13 show comparisons of the P-M interaction diagrams between the theoretical calculation and the experimental results for the four groups of specimens.

For 25 mm and 50 mm eccentrically loaded specimens, bending moment capacities (M_I) were calculated by multiplying the maximum axial load capacity (P_{max}) and the corresponding eccentricity (e). Secondary bending moments (M_{II}) were also calculated as follows:

$$M_{II} = P_{\max}(e + \delta) \quad (1)$$

where δ is the corresponding lateral deflection at the maximum load P_{max}.

From Figures 10 - 13, it can be seen that the theoretical calculations were in good agreement with the experimental results. With the exception of Specimens HF-0 and HF-50, the theoretical results underestimated the experimental results for all of the specimens. For unwrapped specimens there were about 2% to 5% differences between the theoretical and the experimental results. VHF specimens and AHF specimens showed differences of 5.0% to 10.5% and 3.8% to 8.4%, respectively. Specimen HF-0, which got premature failure during concentric testing process showed -3.2 % difference from the theoretical prediction and that for Specimen HF-50 was -7.3% (the minus sign here denotes the experimental results were lower than the calculated results). Specimen HF-25 showed 10% difference compared with theoretical calculation.

The theoretical strain results of reinforcement were also compared with the data obtained from strain gages showing good predications. Two types of strain gages were used: PFL-10-11-1LJB (10 mm length, 2% limit strain) was used for longitudinal steel bars, FLA-11-1L (5 mm length, 1% limit strain) for ties. Details of arrangement of strain gages are given in Fig. 14.

Table 6 shows the strain of longitudinal steel bars from strain gages and compared with the theoretical calculations at maximum load for all of the specimens under concentric loading, 25 mm and 50 eccentricities. For concentric loading, the theoretical strain of steel bars was assumed to have yielded and equal to 2900 με. The experimental strain was taken by the average value of four strain gages glued on the four longitudinal steel bars. The strain of Specimen RC-0 showed 8.8% difference compared to the theoretical calculation, meanwhile Specimens VHF-0 and AHF-0 were 14% and 15.4%, respectively. The

longitudinal steel bars strain of Specimen HF-0 was not applicable here because of the variation due to premature failure.

In case of eccentric loading, the theoretical strains of longitudinal steel bars were carried out for the steel bars on the tension side and compression side based on the principles of strain compatibility and were controlled by concrete strain at maximum load ε_{cc} and the effective strain in FRP ε_{fe}. The strains in the steel bars on the compression side of unwrapped Specimens RC-25 and RC-50 showed about 27% difference compared to theoretical calculation, while those differences for Specimens HF and VHF were between 12% and 20%. Specimens AHF-25 and AHF-50 showed differences of 32% and 27.2%, respectively. The strain in the steel bars on the tension side showed very good agreement with the theoretical calculations for 50 mm eccentric loading. At this eccentricity, the theoretical strain of the tensile steel layer is equal to zero. For 25 mm eccentric loading, the strain in the tensile steel bars showed large differences compared to the theoretical calculations. These strain values in fact were very small, which may have been caused by inaccuracy.

The strain in ties in both tension and compression sides were also measured and are given in Table 7. It is to be noted that in cases of concentric loading or when the eccentricity was small (25 mm), the strain in the ties of all the specimens was significant at maximum load, but the ties had not yielded yet. Therefore, it is necessary to take the contribution of ties into account in calculating the strength of confined concrete in the cases where the stress-strain curves are of the descending types and the ties have been still working. When the eccentricity was large (50 mm), the strain of ties decreased considerably. The fact that up to the yield point of the steel, no differences exist in the confinement mechanism between steel and FRP as they both behave in a linear elastic way. This may explain the inefficiency of FRP under large eccentric loading where the premature failure due to bending moment dominates the

failure modes of the specimens. In addition, at the tension side when the strain of longitudinal steel bars were close to zero, the strain of tie at that side was also close to zero.

5. Conclusions

In order to investigate the effect of fibre orientation on hollow core square reinforced concrete columns confined with Carbon fibre-reinforced polymer, three orientations of fibre wrapping were used and tested on twelve specimens under both concentric and eccentric conditions. From the test results, the following conclusions are drawn:

The fibre in the hoop direction can significantly increase the ductility of hollow core square reinforced concrete columns under concentric or eccentric loading. Compared to VHF and AHF columns, HF columns can sustain much larger deformation before failure. However, the increment of the compressive strength of FRP-confined hollow core columns is marginal.

When columns were tested under eccentric loading, the contribution of vertical and $\pm 45^{\circ}$ angle layers was evident in resisting the bending moment. This contribution was more noticeable as the eccentricity increased. In fact, Specimens AHF-50 and VHF-50, which were wrapped with one and two hoop CFRP layers gained maximum axial load even greater than that of Specimen HF-50, which was wrapped with three CFRP layers in the hoop direction. There is no contribution of these vertical and angle wraps on the strength of columns under concentric loads.

In this paper, the combination of $\pm 45^{o}$ oriented CFRP layers and one hoop layer did not show any significant increase in deflections of the columns under both concentric and eccentric testing. Possible reason is that the contribution of axial loading is more than that of bending in this experiment.

Although Mander et al.'s stress-strain model (1988) is for solid rectangular RC columns, the theoretical calculations using this model for predicting the strength of the tested specimens were in good agreement with the experimental results. The selection of Mander et al.'s model (1988) in this paper was based on the shape of the stress-strain curves of the tested specimens. In the authors' opinion, when a column shows a stress-strain curve of ascending type, which is similar to that of Mander et al.'s model (1988), the behaviour of that column is similar to specimens studied by Mander et al. (1988).

Finally, all of the three wrapping combinations used in this study increased the performance of hollow core square columns. The enhancement in ductility was more evident than the enhancement in strength for all types of wrapping, in particular for columns wrapped with only hoop-oriented layers.

Acknowledgement

The authors would like to thank staff at the High Bay laboratory, University of Wollongong, especially Mr. Fernando Escribano for their technical help during the experimental program. Thanks are expressed to PhD scholar Mr. Ida Bagus Rai Widiarsa for his design of loading heads, which used in this experiment. Finally, the second author would like to acknowledge Hong Duc, Thanh Hoa, Vietnam and UOW Research Scholarship Program for the support of his full Masters scholarship.

References

[1] Li J, Hadi MNS. Behaviour of externally confined high-strength concrete columns under eccentric loading. Composite Structures 2003;62(2):145-153.

[2] Hadi MNS. Comparative study of eccentrically loaded FRP wrapped columns. Composite Structures 2006;74(2):127-135.

[3] Hadi MNS. Behaviour of FRP wrapped normal strength concrete columns unde eccentric loading. Composite Structures 2006;72(4):503-511.

[4] Fitzwilliam J, Bisby L. Slenderness effects on circular CFRP confined reinforced concrete columns. Journal of Composites for Construction 2010;14(3):280-288.

[5] Hadi MNS. Behaviour of FRP strengthened concrete columns under eccentric compression loading. Composite Structures, 2007;77(1):92-96.

[6] Hadi MNS, Widiarsa IBR. Axial and Flexural Performance of Square RC Columns Wrapped with CFRP under Eccentric Loading Journal of Composites for Construction 2012;16(6):640-649.

[7] Tan KH. Strength enhancement of rectangular reinforced concrete columns using fibre-reinforced polymer. Composites in Construction 2002;6(3):175-183.

[8] Rochette P, Labossiere P. Axial testing of rectangular column models confined with composites. Journal of Composites for Construction 2000;4(3):129-136.

[9] Mirmiran A, Shahawy M. Behaviour of concrete columns confined by fibre composites. Journal of structural engineering New York, N.Y. 1997;123(5):583-590.

[10] Pessiki S, Harries KA, Kestner JT, Sause R, Ricles JM. Axial behaviour of reinforced concrete columns confined with FRP jackets. Journal of Composites for Construction 2001;5(4):237-245.

[11] Li G, Maricherla D, Singh K, Pang S-S, John M. Effect of fibre orientation on the structural behaviour of FRP wrapped concrete cylinders. Composite Structures 2006;74(4):475-483.

[12] Sadeghian P, Rahai AR, Ehsani MR. Effect of Fibre Orientation on Compressive Behaviour of CFRP-confined Concrete Columns. Journal of Reinforced Plastics and Composites 2010;29(9):1335-1346.

[13] Parvin A, Jamwal AS. Effects of wrap thickness and ply configuration on composite-confined concrete cylinders. Composite Structures 2004;67 (2005):437–442.

[14] Parvin A, Jamwal AS. Performance of externally FRP reinforced columns for changes in angle and thickness of the wrap and concrete strength. Composite Structures 2005;73 (2006):451–457.

[15] Hajsadeghi M, Alaee FJ, Shahmohammadi A. Investigation on Behaviour of Square/Rectangular Reinforced Concrete Columns Retrofitted with FRP Jacket. Journal of Civil Engineering and Management 2011;17(3):400-408.

[16] Lignola GP, Prota A, Manfredi G, Cosenza E. Experimental performance of RC hollow columns confined with CFRP. Journal of Composites for Construction 2007;11(1):42-49.

[17] Yazici V, Hadi MNS. Axial load-bending moment diagrams of carbon FRP wrapped hollow core reinforced concrete columns. Journal of Composites for Construction 2009;13(4):262-268.

[18] Kusumawardaningsih Y, Hadi MNS. Comparative behaviour of hollow columns confined with FRP composites. Composite Structures 2010;93(1):198-205.

[19] Han TH, Stallings JM, Cho SK, Kang YJ. Behaviour of a hollow RC column with an internal tube. Magazine of Concrete Research 2010;62(1):25-38.

[20] Han TH, Yoon KY, Kang YJ. Compressive strength of circular hollow reinforced concrete confined by an internal steel tube. Construction and Building Materials 2010;24(9):1690-1699.

[21] Teng JG, Yu T, Wong YL, Dong SL. Hybrid FRP-concrete-steel tubular columns: Concept and behaviour. Construction and Building Materials 2007;21(4):846-854.

[22] Wong YL, Yu T, Teng JG, Dong SL. Behaviour of FRP-confined concrete in annular section columns. Composites Part B: Engineering 2008;39(3):451-466.

[23] Xie P, Yu T, Wong YL, Teng JG. Compressive behaviour of large-scale hybrid FRP-concrete-steel double-skin tubular columns. in 1st International Conference on Civil Engineering, Architecture and Building Materials, CEABM 2011, June 18, 2011 - June 20, 2011. 2011. Haikou, China: Trans Tech Publications.

[24] Yu T, Teng JG. Behaviour of hybrid FRP-concrete-steel double-skin tubular columns with a square outer tube and a circular inner tube subjected to axial compression. Journal of Composites for Construction 2013;17(2):271-279.

[25] Yu T, Teng JG, Wong YL. Stress-strain behaviour of concrete in hybrid frp-concrete-steel double-skin tubular columns. Journal of Structural Engineering 2010;136(4):379-389.

[26] Yu T, Wong YL, Teng JG. Behaviour of hybrid FRP-concrete-steel double-skin tubular columns subjected to eccentric compression. Advances in Structural Engineering 2010;13(5):961-974.

[27] AS 3600-2009. Concrete structure. Standards Australia Limited, NSW 2009.

[28] Taylor AW, Rowell RB, Breen JE. Behaviour of thin-walled concrete box piers. ACI Structural Journal 1995;92(3):319-333.

[29] ASTM D7565/D7565M – 10. Standard Test Method for Determining Tensile Properties of Fibre Reinforced Polymer Matrix Composites Used for Strengthening of Civil Structures. ASTM International, United States 2010.

[30] AS 1012.8-2000. Methods of testing concrete. Standards Australia International Ltd., NSW 2000.

[31] AS 1012.9-1999. Methods of testing concrete. Standards Australia International Ltd., NSW 1999.

[32] AS 1391-2007. Metallic materials - Tensile testing at ambient temperature. Standards Australia Limited, NSW 2007.

[33] GangaRao HVS, Taly N, Vijay PV, Reinforced concrete design with FRP composites. 2007: New York : CRC ; London : Taylor & Francis.

[34] Warner RF, Foster SJ, Kilpatrick AE. Reinforced concrete basics : analysis and design of reinforced concrete Pearson Prentice Hall, Frenchs Forest, N.S.W 2007.

[35] Mander JB, Priestley MJN, Park R. Theoretical stress-strain model for confined concrete. Journal of structural engineering New York, N.Y. 1988;114(8):1804-1826.

[36] ACI 440.2R. Guide for the Design and Construction of Externally Bonded FRP Systems for Strengthening Concrete Structures. American Concrete Institute, Farmington Hills, USA 2002.

[37] ACI 440.2R. Guide for the Design and Construction of Externally Bonded FRP Systems for Strengthening Concrete Structures. American Concrete Institute, Farmington Hills, USA 2008.

[38] Lam L, Teng JG. Design-oriented stress-strain model for FRP-confined concrete in rectangular columns. Journal of Reinforced Plastics and Composites 2003;22(13):1149-1186.

[39] Carey S, Harries K. The Effects of Shape, 'Gap', and Scale on the Behaviour and Modeling of Variably Confined Concrete. Report No. ST03-05, University of South Carolina, Columbia, SC 2003.

[40] Toutanji H, Han M, Gilbert J, Matthys S. Behaviour of large-scale rectangular columns confined with FRP composites. Journal of Composites for Construction 2010;14(1):62-71.

List of Figures

List of □□□es

Table

Table 1
FRP coupon test results

Configuration	1 layer	2 layers	3 layers
Width, mm	23.9	24.7	25.3
Gage length, mm	138	138	138
Maximum tensile force before failure, N	13785	25891	38370
Maximum displacement, mm	2.058	2.075	2.398
Maximum tensile force per unit width, N/mm	1165.3	1150.7	1136.9
Maximum strain	0.0149	0.0185	0.0174
Tensile modulus of elasticity, MPa	78080	76503	65310

Table 2
Configuration of specimens

Specimen [1]	Internal reinf.	Configuration CFRP	Eccentricity mm
RC-0			0
RC-25	Yes	None	25
RC-50			50
HF-0		Three	0
HF-25	Yes	hoop	25
HF-50		layers	50
VHF-0		One vertical	0
VHF-25	Yes	and two hoop	25
VHF-50		layers	50
AHF-0		Two ($\pm 45^0$)	0
AHF-25	Yes	and one hoop	25
AHF-50		layers	50

[1]All specimens have the dimensions 200x200 mm in cross-section and 800 mm in height.

Table 3
Summary of testing results

Specimen	Max. load	Corresponding displacement at max. load		Ultimate displacement		Corr. axial load at ultimate displacement	Normalized max. load
		Axial	Lateral	Axial	Lateral		
	kN	mm	mm	mm	mm	kN	
RC-0	1341	3.32	N/A[1]	3.58	N/A	1139	1
HF-0	1485	21.99	N/A	-	-	-[2]	1.11
VHF-0	1525	4.03	N/A	8.07	N/A	1287	1.14
AHF-0	1417	3.81	N/A	7.02	N/A	1174	1.06
RC-25	998	2.99	1.71	3.15	1.99	848	1
HF-25	1245	3.75	1.48	-	-	-	1.25
VHF-25	1189	3.80	1.57	8.17	6.14	911	1.19
AHF-25	1083	3.73	2.29	7.60	7.01	759	1.09
RC-50	755	3.06	2.20	3.38	2.70	641	1
HF-50	825	3.67	2.56	26.96	27.94	697	1.09
VHF-50	889	4.13	3.23	10.32	8.34	737	1.18
AHF-50	862	3.78	2.50	8.79	6.65	696	1.14

[1]The lateral displacement is not applicable in cases of concentric loading

[2]Data was lost due to an accident during testing

Table 4
Calculation of ductility

Specimen	Axial displacement (mm)		Ductility	Normalized ductility
	at yield load	at 85% P_{max}		
	Δ_y	$\Delta_{85\%Pmax}$	$\Delta_{85\%Pmax}/\Delta y$	
RC-0	2.80	3.58	1.3	1.0
HF-0	3.83	22.98	6.0	4.7
VHF-0	2.92	8.05	2.8	2.2
AHF-0	2.75	6.76	2.5	1.9
RC-25	2.62	3.15	1.2	1.0
HF-25	N/A [1]	N/A	N/A	N/A
VHF-25	2.92	6.07	2.1	1.7
AHF-25	3.05	5.87	1.9	1.6
RC-50	2.59	3.38	1.3	1.0
HF-50	2.78	26.89	9.7	7.4
VHF-50	2.78	8.52	3.1	2.3
AHF-50	2.94	7.89	2.7	2.1

[1]Data was lost due to an accident during testing

Table 5
Summary of theoretical calculations

Group	Eccentricity	Theoretical max. load $P_{theo.}$	Bending moment $M_{theo.}=P_{theo.}e$	Experimental max. load $P_{expt.}$	M_I $=P_{expt.}e$	M_{II} $=P_{expt.}(e+\delta)$	Difference
	mm	kN	kNm	kN	kNm	kNm	%
RC	0	1274	0	1341	0	0	5.3
	25	962	24.1	998	25.0	26.7	3.8
	50	741	37.1	755	37.7	39.4	1.8
HF	0	1535	0	1485	0	0	-3.2
	25	1132	28.3	1245	31.1	33.0	10.0
	50	890	44.5	825	41.3	43.4	-7.3
VHF	0	1452	0	1525	0	0	5.0
	25	1076	26.9	1189	29.7	31.6	10.5
	50	845	42.3	889	44.4	47.3	5.2
AHF	0	1366	0.00	1417	0	0	3.8
	25	1018	25.5	1083	27.1	29.6	6.4
	50	795	39.8	862	43.1	45.2	8.4

Table 6
Theoretical and experimental strains of longitudinal steel bars at maximum load

Specimen	Strain of bars in compression side (με) (Average value of SG3 and SG4)			Strain of bars on tension side (με) (Average value of SG1and SG2)		
	Theo.	Exp.	Difference (%)	Theo.	Exp.	Difference (%)
RC-0	2900	3156	8.8			
RC-25	2420	3073	27.0	213	354	66.2
RC-50	2390	3044	27.4	0	29	≅0 [1]
HF-0	2900	N/A	N/A			
HF-25	3880	3149	-18.8	926	856	-7.6
HF-50	3730	4302	15.3	0	16	≅0
VHF-0	2900	3305	14.0			
VHF-25	3124	3501	12.1	263	358	36.1
VHF-50	3080	3698	20.1	0	57	≅0
AHF-0	2900	3346	15.4			
AHF-25	2621	3477	32.0	234	447	91.0
AHF-50	2550	3243	27.2	0	12	≅0

[1]The experimental strains of bars SG1, SG2 at 50 mm eccentric loading were very close to zero.

Note: Refer to Fig. 12 for locations of Strain Gages SG1 – SG4

Table 7
Strain of the tie at mid-height of column (Strain gages SG5 and SG6)

Specimen	At yield load (με)		At max. load (με)		At 85% of max. load (με)		At load corr. to ultimate strain (με)	
	SG5	SG6	SG5	SG6	SG5	SG6	SG5	SG6
RC-0	752	563	1261	770	2761	956	2761	956
HF-0	1129	450	1861	1599	10237	8987	failed [1]	failed
VHF-0	913	593	1413	935	1298	888	1125	860
AHF-0	960	639	1915	1234	2448	1517	2421	1448
RC-25	130	786	135	1153	97	1257	97	1257
HF-25	N/A	N/A [2]	158	1426	N/A	N/A	79	1347
VHF-25	79	- [3]	91.6	-	82	-	76	-
AHF-25	82	696	101	1356	362	838	472	724
RC-50	13	592	13	813	7	841	7	841
HF-50	10	520	19	856	207	1156	204	1150
VHF-50	8	531	19	820	19	808	21	714
AHF-50	0	546	2	749	27	758	36	730

[1]At that point the strain gage already reached limit strain value (1% for strain gages glued on tie) and failed.
[2]The strain gage values were not applicable because Specimen HF-25 got accident during testing.
[3]The strain gage broke.
Note: Refer to Fig. 12 for locations of Strain Gage SG5 and SG6

Figure 1

Figure 1

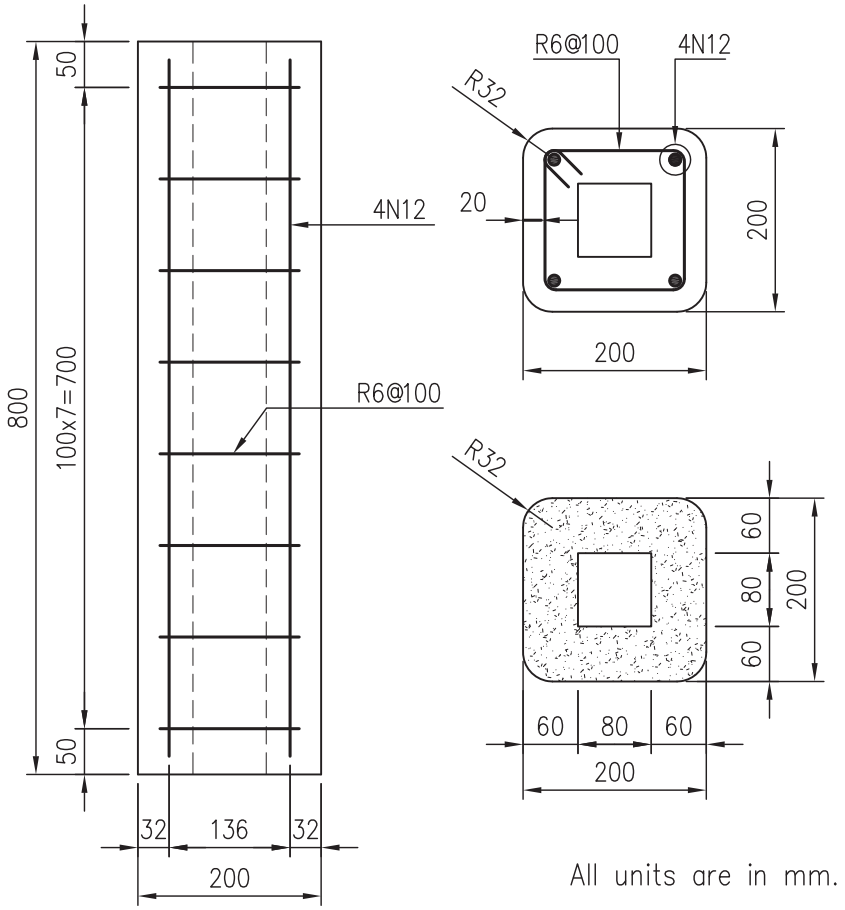

Figure 2

Figure □

Figure 3

Figure 3

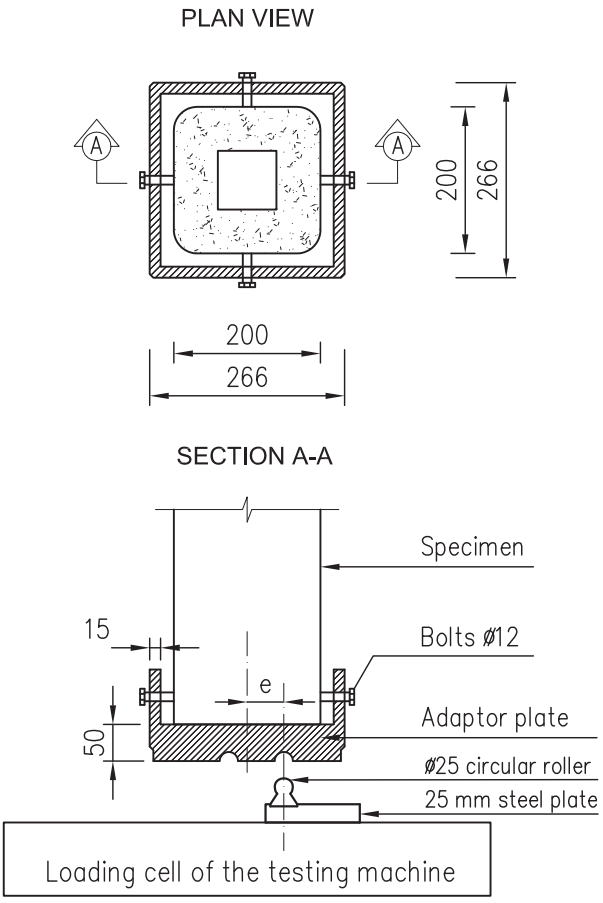

Figure 4

Figure 4

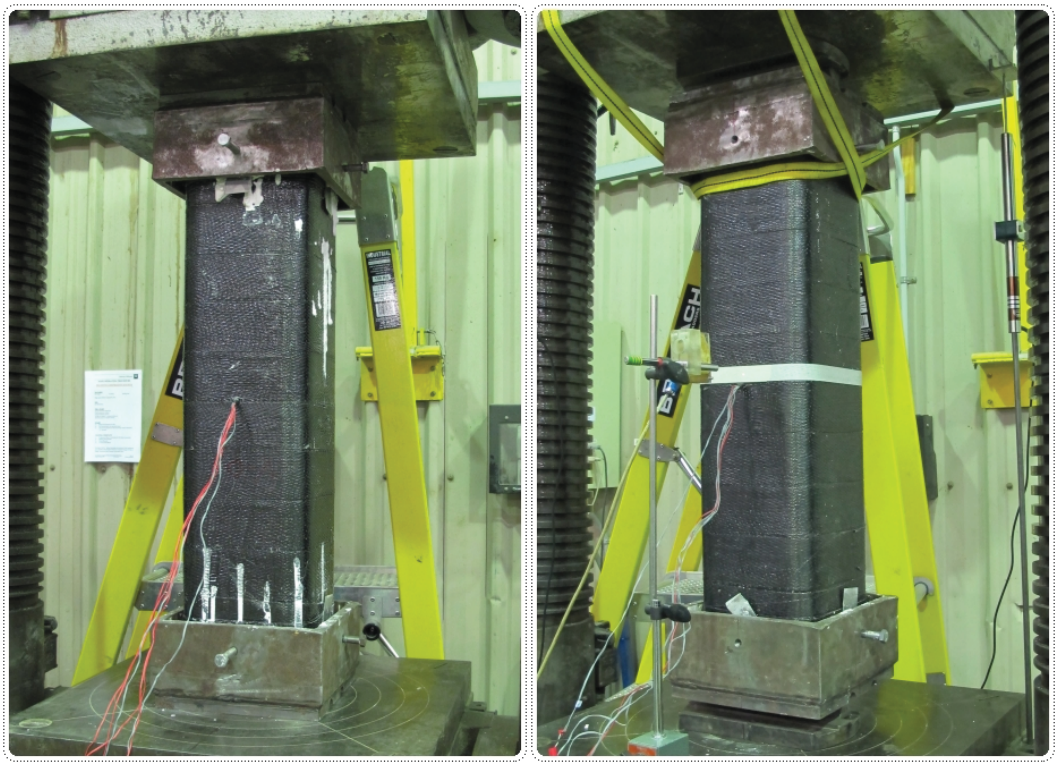

A concentrically loaded specimen

An eccentrically loaded specimen

Figure

Figure 5

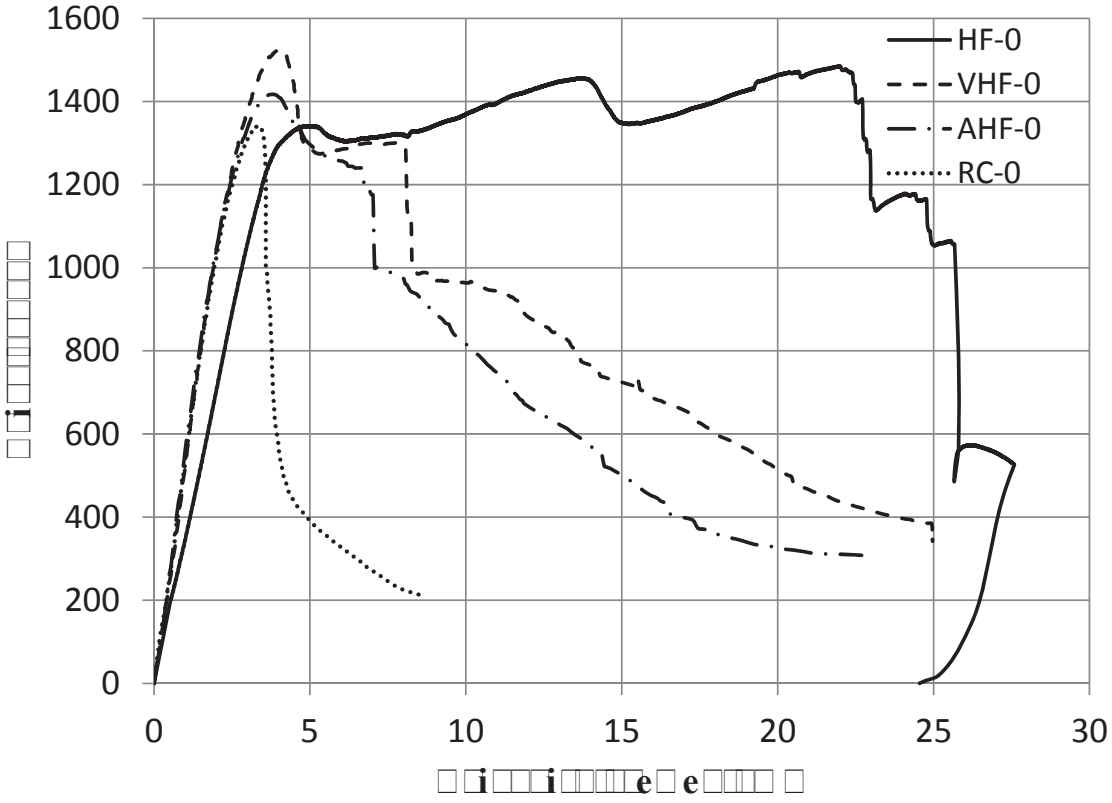

Figure 6

Figure 6

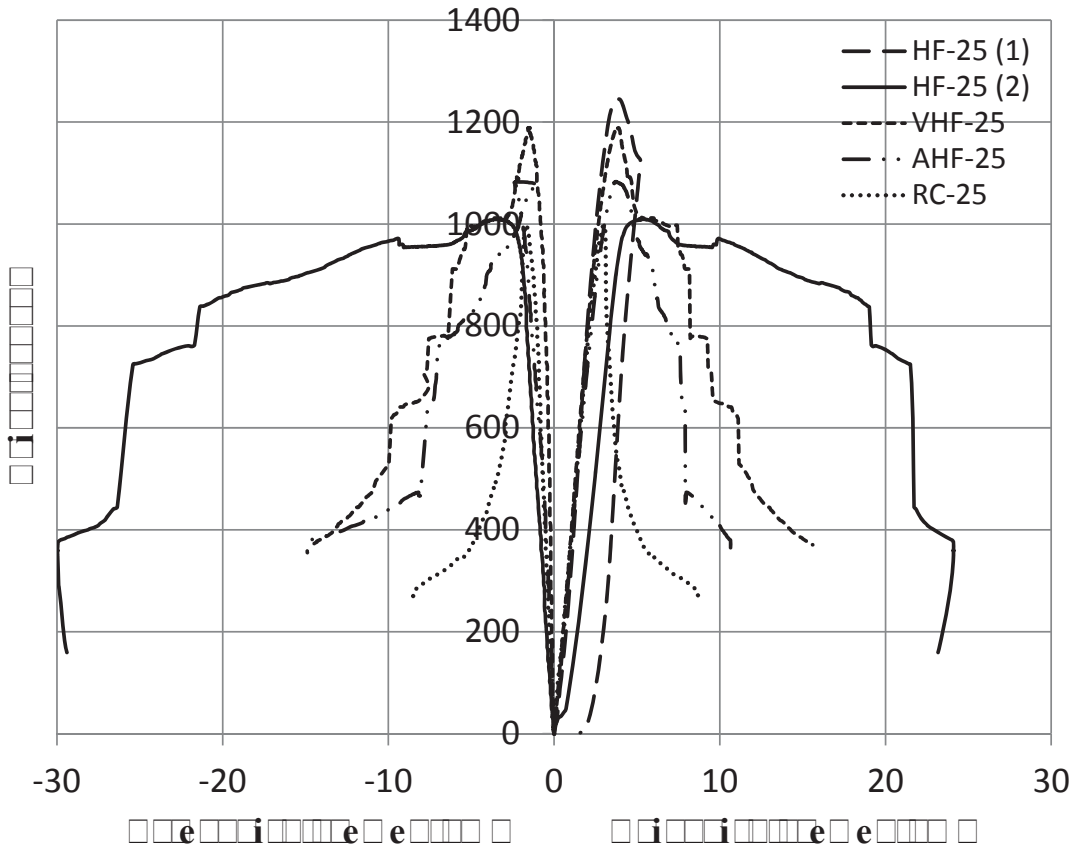

Figure 7

Figure 5

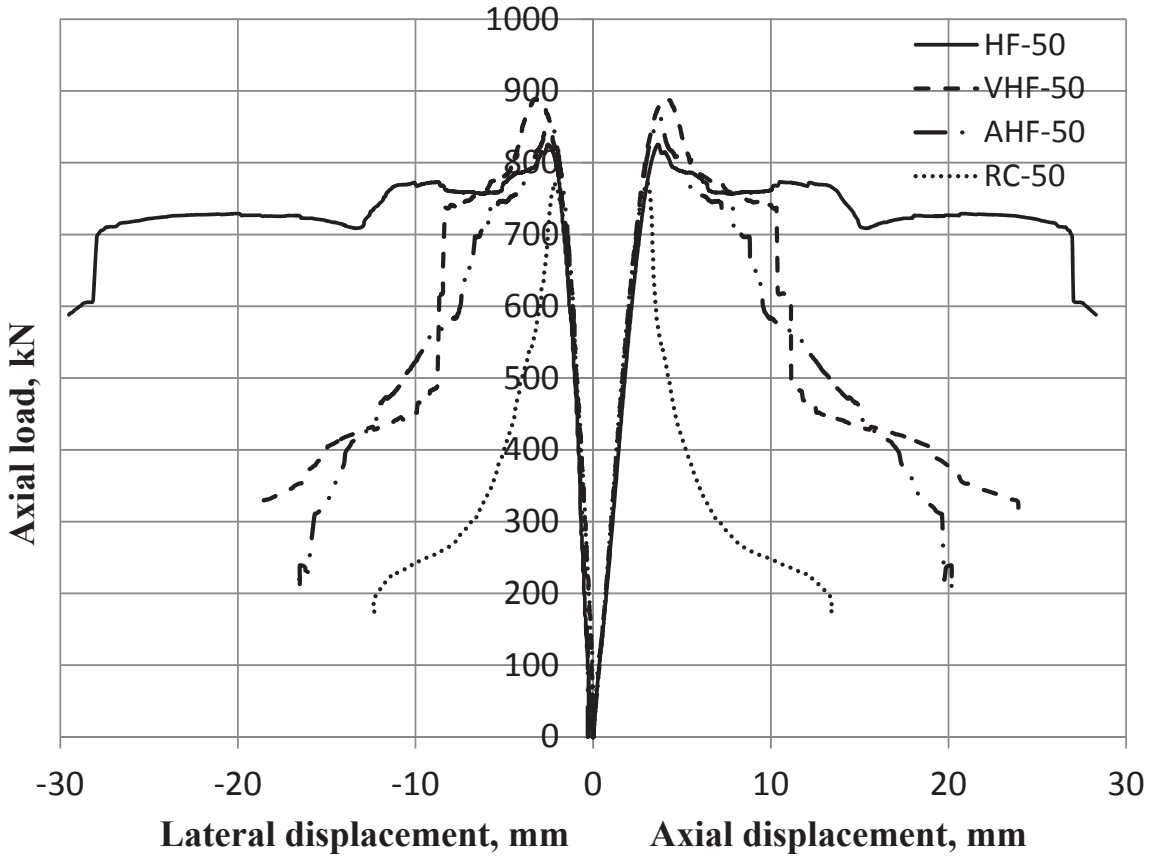

Figure 8

□i□□re 8

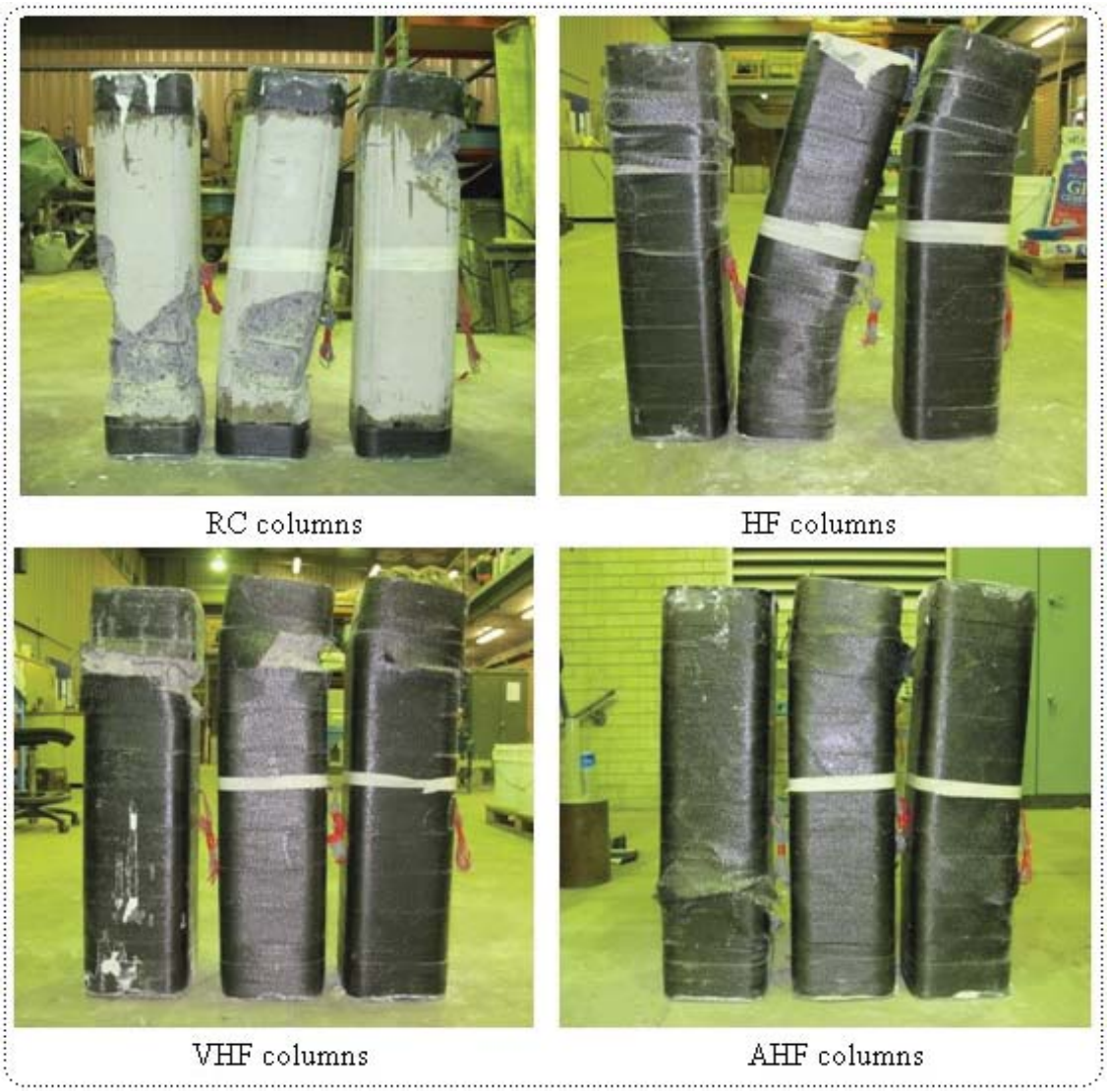

Figure 9

□i□□re 9

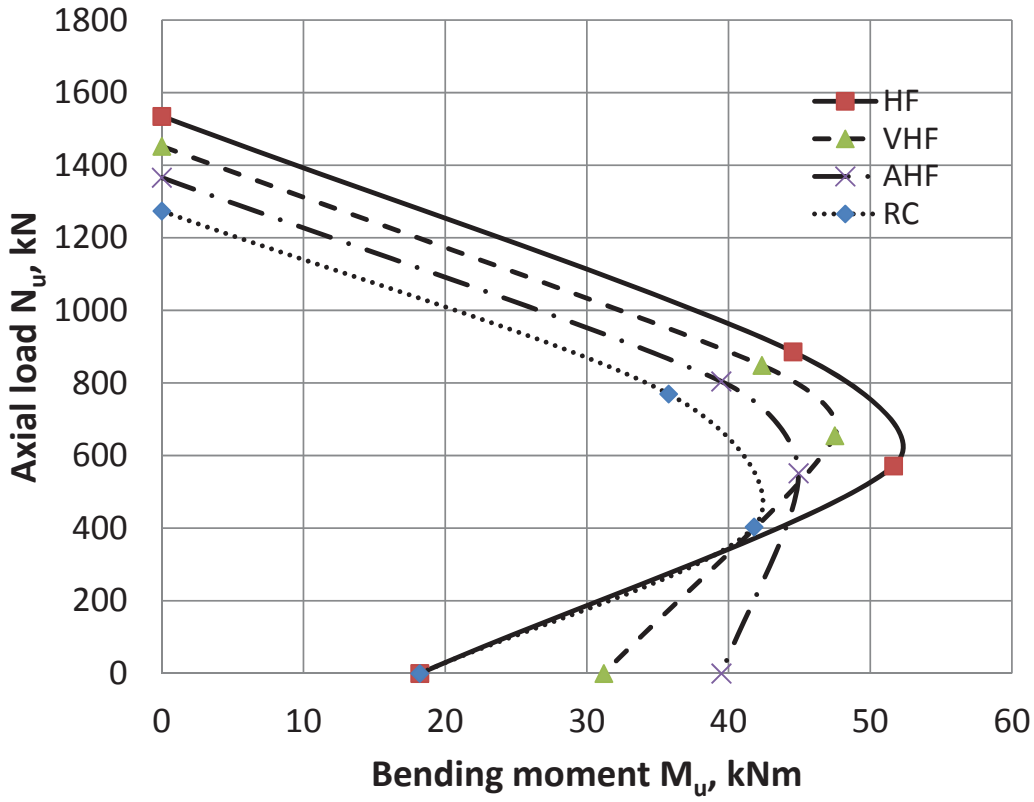

Figure 10

□i□□re 10

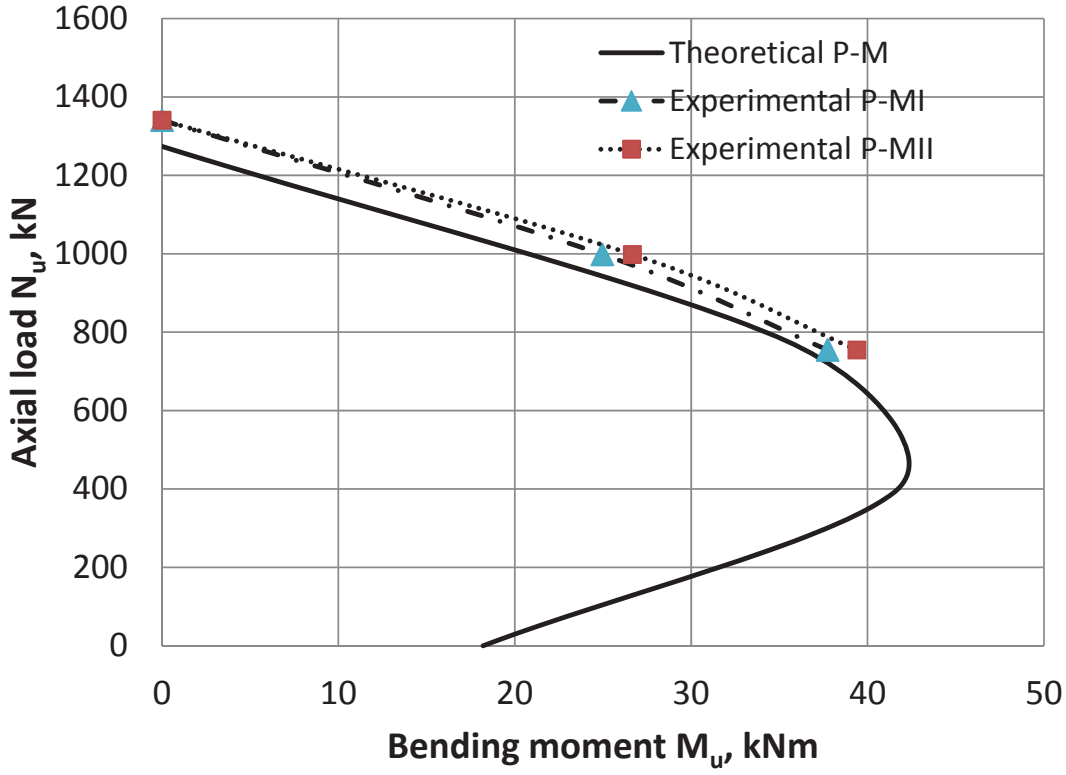

Figure 11

□i□□re 11

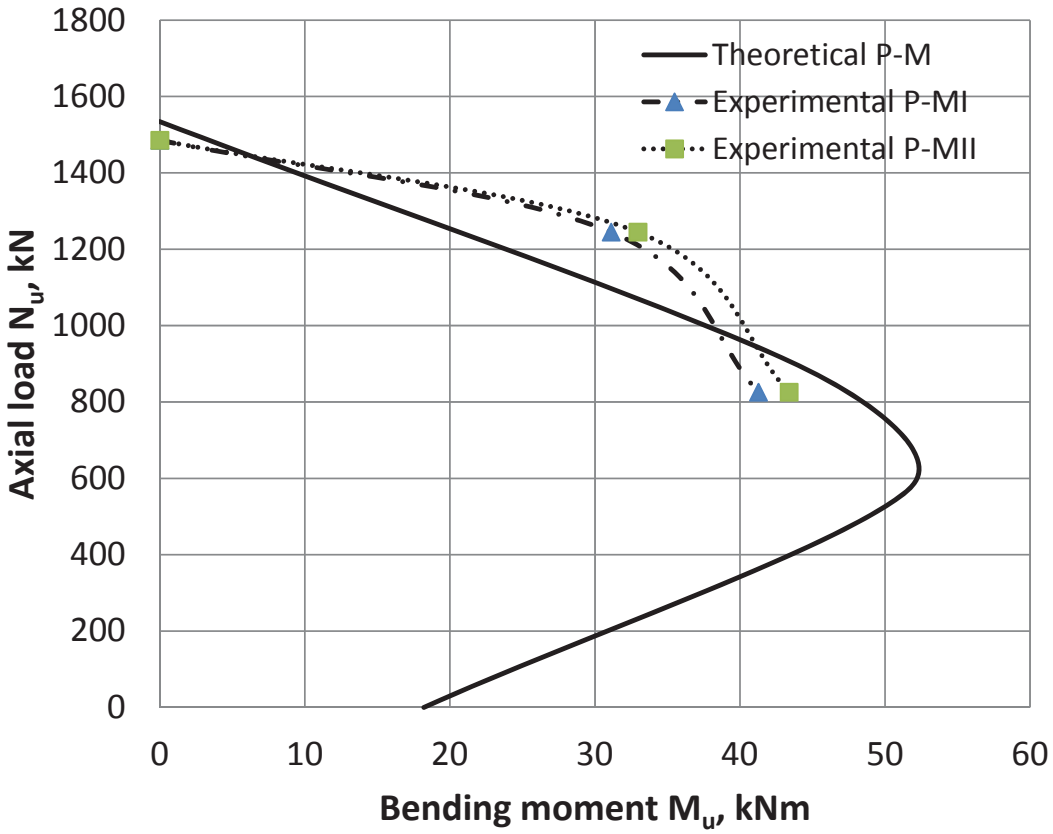

Figure 12

Figure 12

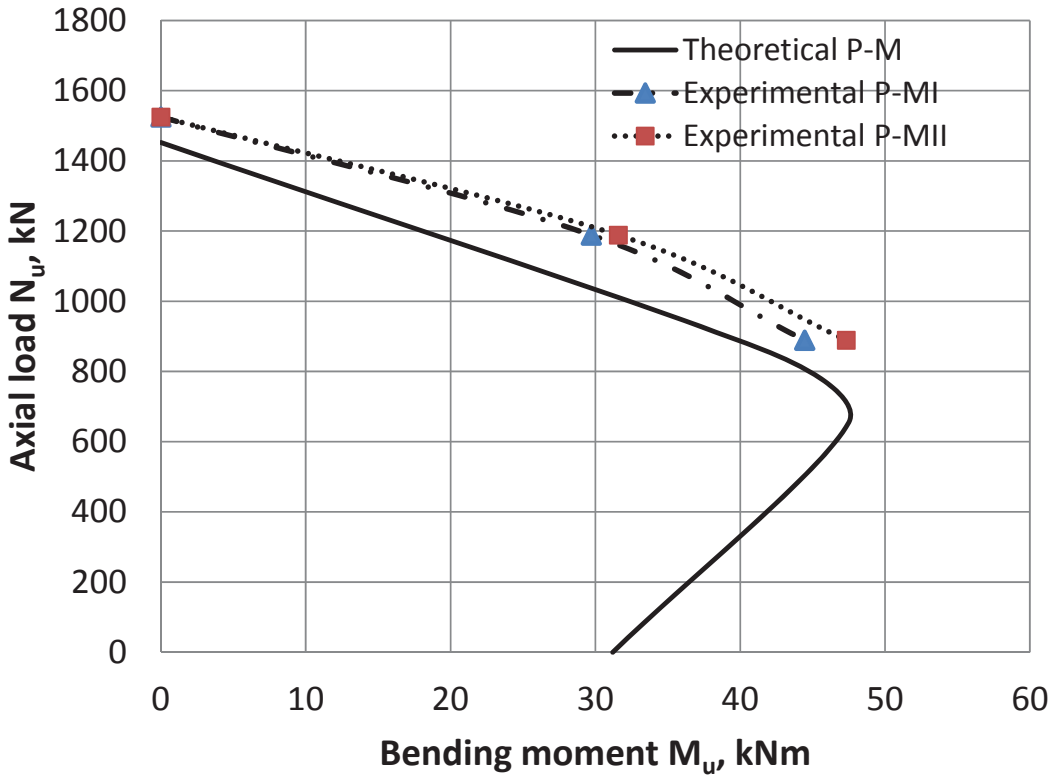

Figure 13

Figure 13

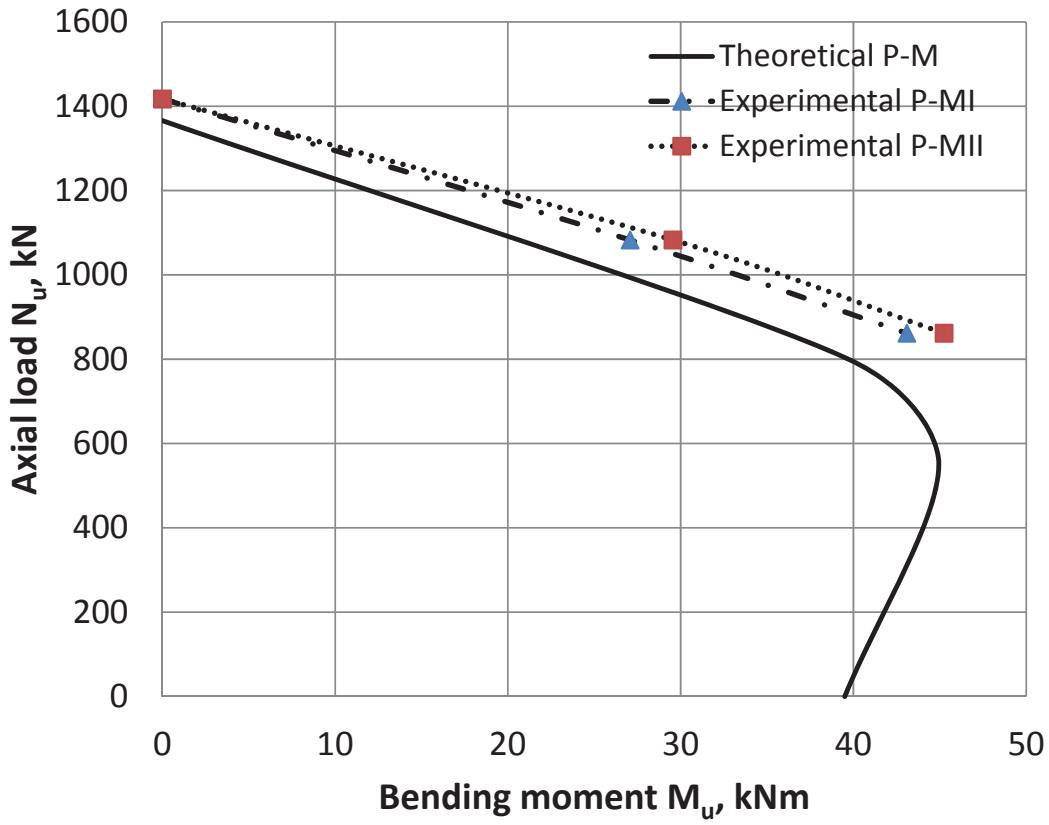

Figure 14

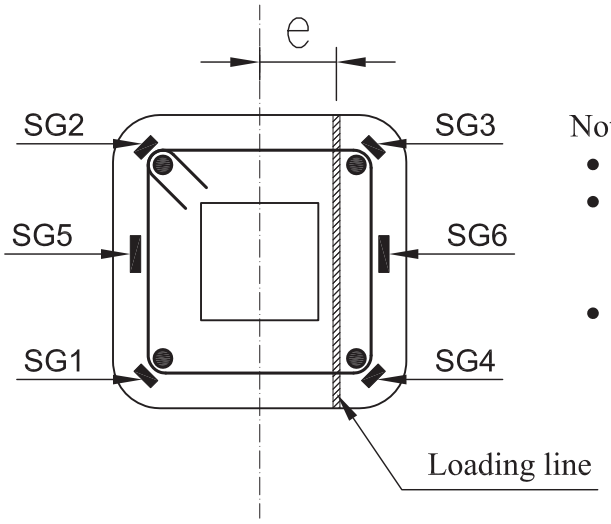

Notes:

- e is the eccentricity
- Strain gages SG1, SG2, SG3, SG4 were placed on at mid-height of longitudinal steel bars
- Strain gages SG5, SG6 were placed on a tie at mid-height of the column